COBEM 2023 27TH INTERNATIONAL CONGRESS OF MECHANICAL ENGENEERING

ABCM Brazilian Society of Mechanical Sciences and Engineering
27th ABCM International Congress of Mechanical Engineering
December 04-08, 2023, Florianópolis-SC, Brazil

COB-2023-0518
WAVE PROPAGATION AND BAND GAP FORMATION IN CORRUGATED PLATES

Rodrigo Nicoletti
University of São Paulo, São Carlos School of Engineering, Trabalhador São Carlense 400, 13566-890 São Carlos, SP, Brazil
rnicolet@sc.usp.br

Abstract. *Structures with geometric periodicity can present interesting dynamic properties like stop and pass frequency bands. Hence, by adopting such structures, one can design systems that present minimum dynamic response in a given frequency range with large bandwidth. In the present work, it is shown that corrugated plates also present the dynamic properties of periodic structures due to their periodic geometry only. Periodic corrugation is the plastic deformation of the plate into given shapes whose patterns repeat in the two-dimensional space of the plate. Hence, in this case, there is no need of changing the mass or material properties along the structure (a common approach found in the literature) to form stop band regions in the frequency spectrum. The corrugated plate is modeled by finite elements and the resultant dispersion diagrams (out-of-plane vibration) are obtained using the COMSOL software. The results show that band gaps indeed appear in the frequency spectrum of the plate. In addition, the bandwidth and the central frequency of the band gap depend on the direction of propagation of the vibrating wave. The corrugated shape of the plate can differ from one direction to the other in the two-dimensional space of the plate and, depending on the corrugation density in a given direction of propagation, different stop band regions form in the frequency spectrum. The obtained results show that one can tailor the band gaps in the orthogonal directions of propagation by changing the corrugation shape of the plate.*

Keywords: *periodic structures, metamaterials, wave dispersion, mechanical vibration, wave attenuation*

1. INTRODUCTION

Periodic structures have interesting dynamic characteristics that can be usefully explored in the design of mechanical systems. The most important characteristic of such systems is the presence of stop-band zones in their frequency spectrum. Such zones (also called band gaps) are frequency regions where mechanical waves cannot propagate (or are strongly attenuated). Hence, we can design the structure to present periodic geometry or material distribution to create such band gaps in frequency regions of interest. This idea has gained researchers' attention in the last decade, and several studies were conducted focusing on how periodicity affects the dynamics of 1D (bars, rods, and beams), 2D (membranes and plates), and 3D (solids and lattices) structures.

In the area of 2D structures, the first ideas came with the help of PZT patches (piezoelectric actuators). In the beginning, the use of PZT patches distributed over the surface of the plate aimed at controlling vibration in an active or semi-active way (Casadei *et al.*, 2010; Nouh *et al.*, 2016). However, when these patches were periodically distributed over the surface, one observed that large band gaps appeared in the frequency response functions of the structure. This led to the adoption of local resonators not based on PZT patches, but based on simple spring-mass systems (Song *et al.*, 2015; Zouari *et al.*, 2017). It has been proven that local resonators periodically mounted on the surface of plates result in not only large band gap regions but also complete band gaps in the irreducible Brillouin zone. This has been verified both numerically and experimentally, and the band gap can be designed to a specific frequency region by adopting optimization procedures (Xiong *et al.*, 2023).

An alternative way of creating a periodic 2D structure is distributing its inertia periodically. This can be achieved by mounting inserts on the surface of the plate (Zhang *et al.*, 2012) or by changing the thickness of the plate (Poggetto and Arruda, 2021). In the case of the periodic variation of the thickness plate, one can create complete band gaps in the Brillouin zone by optimizing the shape of the plate thickness. In this case, spatial Fourier coefficients can be used to represent the thickness distribution of the plate in the unit cell of the periodic structure (Poggetto and Arruda, 2021). A different approach is the topological optimization of the structure, where the local thickness is defined by the optimization procedure (El-Sabbagh *et al.*, 2008)

The inertia can also be periodically distributed on 2D structures by removing material. In this case, holes of different geometry (squared, rectangular, circular) are machined in the plate in a periodic distribution (Das *et al.*, 2020; Guo *et al.*, 2022). Such a strategy results in non-complete band gaps in the Brillouin zone (directional band gaps) in the Γ-X and M-Γ planes. It was observed both numerically and experimentally that the band gap widens (increases its bandwidth) when the aspect ratio of the hole decreases (Das *et al.*, 2020). It was also observed that the adoption of rib stiffeners led to the appearance of complete band gaps (Guo *et al.*, 2022).

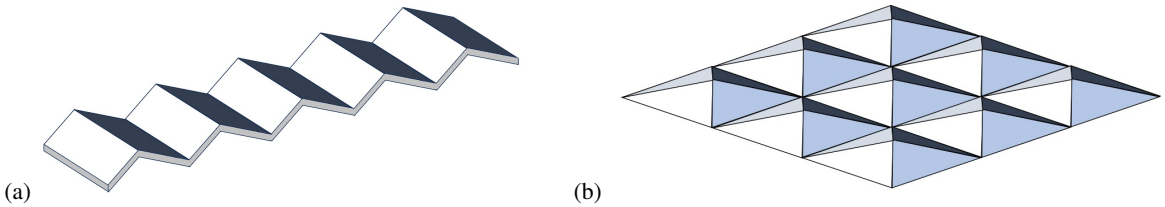

(a) (b)

Figure 1. Examples of corrugated structures: (a) corrugated beams with straight segments, (b) corrugated plate with straight faces (pyramidal bumps).

Stiffeners (ribs) can also be mounted periodically on the surface of the plate and result in the formation of band gaps. In fact, as one increases the stiffness ratio between the plate and the stiffener, it is possible to create complete band gaps in the irreducible Brillouin zone (Wang *et al.*, 2012; Guo *et al.*, 2022). By altering the periodic distances or dimensions of the attached structures, the radiated pressure of the stiffened plate can be effectively adjusted at different frequencies (Zhou *et al.*, 2020).

The structure can also present band gaps when its geometry is periodically corrugated, i.e. the structure presents periodic bumps imposed by plastic deformation. For example, a beam with corrugated geometry (1D structure – Fig. 1a) presents band gaps in its frequency spectrum, and the band gap width increases with the number of bumps in the beam Bachour and Nicoletti (2021). In this case, impedance mismatch shifts the upper frequency of the band gap, which is usually associated with localized mode shapes of the straight segments of the beam. The band gaps appear in such corrugated structures with segment angles above 2.5 degrees.

As we can see in the literature review, most of the periodic structures analyzed in the literature involve some sort of modification of the mass or the material property along the structure. In the case of corrugated beams, no such modification is needed, because the beam is shaped in the corrugated geometry, keeping the same material properties and the cross-sectional area along the beam (the geometry does the work). That represents an advantage from a manufacturing standpoint. Considering this, the present work extends the analysis of corrugated beams to corrugated plates (2D structures). In this case, the 2D structure (plate) is corrugated with straight faces, thus resulting in a periodic sequence of pyramid-shaped bumps in both perpendicular directions (Fig. 1b). It is important to note that this is still a plate with a constant thickness at every face of the corrugation. The corrugated plate is modeled by finite elements and the resultant dispersion diagrams (out-of-plane vibration) are obtained using the COMSOL software. The results show that band gaps indeed appear in the frequency spectrum of the plate. In addition, the bandwidth and the central frequency of the band gap depend on the direction of propagation of the vibrating wave. The corrugated shape of the plate can differ from one direction to the other in the two-dimensional space of the plate and, depending on the corrugation density in a given direction of propagation, different stop band regions form in the frequency spectrum. The obtained results show that one can tailor the band gaps in the orthogonal directions of propagation by changing the corrugation shape of the plate.

2. MATHEMATICAL BACKGROUND

The corrugated plate in the analysis is a periodic structure. Hence, one can find regions of the structure that repeat periodically. Such regions are called *unit cells*, and one can find the equations of motion of the cell by adopting the finite element model. Hence, the equations of motion of the cell in the global coordinate system, written in the frequency domain, are given by:

$$\left(\mathbf{K}_c - \omega^2 \mathbf{M}_c\right) \mathbf{q}_c(\omega) = \mathbf{D}(\omega)\, \mathbf{q}_c(\omega) = \mathbf{f}_c(\omega) \tag{1}$$

where $\mathbf{M}_c$ and $\mathbf{K}_c$ are the inertia and stiffness matrices of the cell in the global coordinate system, $\mathbf{q}_c$ is the vector of degrees-of-freedom of the system, and $\mathbf{f}_c$ is the vector of external forces.

By rearranging the order of the degrees of freedom, one can separate the boundary and the internal degrees of freedom, in such a way that:

$$\mathbf{q}_c = \left\{ \begin{array}{cccccccccc} \mathbf{q}_L & \mathbf{q}_R & \mathbf{q}_T & \mathbf{q}_B & \mathbf{q}_{LB} & \mathbf{q}_{LT} & \mathbf{q}_{RT} & \mathbf{q}_{RB} & \mathbf{q}_I \end{array} \right\}^T \tag{2}$$

$$\mathbf{f}_c = \left\{ \begin{array}{cccccccccc} \mathbf{f}_L & \mathbf{f}_R & \mathbf{f}_T & \mathbf{f}_B & \mathbf{f}_{LB} & \mathbf{f}_{LT} & \mathbf{f}_{RT} & \mathbf{f}_{RB} & \mathbf{f}_I \end{array} \right\}^T \tag{3}$$

where subscripts L and R refer to the degrees of freedom at the left and right boundaries of the cell, T and B refer to the degrees of freedom at the top and bottom boundaries of the cell, LB, LT, RB, and RT refer to the degrees of freedom at the corner boundaries of the cell, and subscript I refer to the internal degrees of freedom of the cell (Fig. 2).

Due to the periodicity of the structure, the degrees of freedom at the right boundary are related to those at the left

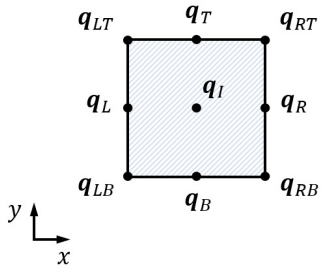

Figure 2. Inner and boundary degrees-of-freedom of the unit cell.

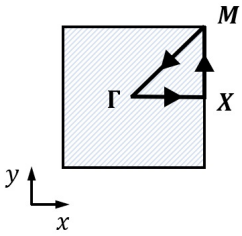

Figure 3. Irreducible Brillouin zone of the unit cell.

boundary by the wavenumber of the propagating wave along the structure (Bloch's theorem – Ruzzene *et al.* (2002)):

$$\begin{cases} \mathbf{q}_R = e^{-\mu_x L_x}\ \mathbf{q}_L \\ \mathbf{q}_T = e^{-\mu_y L_y}\ \mathbf{q}_B \\ \mathbf{q}_{RB} = e^{-\mu_x L_x}\ \mathbf{q}_{LB} \\ \mathbf{q}_{TL} = e^{-\mu_y L_y}\ \mathbf{q}_{LB} \\ \mathbf{q}_{RT} = e^{-\mu_x L_x - \mu_y L_y}\ \mathbf{q}_{LB} \end{cases} \qquad \begin{cases} \mathbf{f}_R + e^{-\mu_x L_x}\ \mathbf{f}_L = \mathbf{0} \\ \mathbf{f}_T + e^{-\mu_y L_y}\ \mathbf{f}_B = \mathbf{0} \\ \mathbf{f}_{RB} + e^{-\mu_x L_x}\ \mathbf{f}_{LB} = \mathbf{0} \\ \mathbf{f}_{TL} + e^{-\mu_y L_y}\ \mathbf{f}_{LB} = \mathbf{0} \\ \mathbf{f}_{RT} + e^{-\mu_x L_x - \mu_y L_y}\ \mathbf{q}_{LB} = \mathbf{0} \end{cases} \tag{4}$$

where μ_x and μ_y are the wavevectors in the x and y directions, and L_x and L_y are the dimensions of the cell in the x and y directions. The real part of μ_x and μ_y will show the propagating frequency regions of the periodic structure, whereas the imaginary part of μ_x and μ_y will show the evanescent frequency regions of the structure.

Hence, by applying Eq.(4), one can rewrite and condensate the vectors of degrees of freedom and force as a function of the left-bottom and internal degrees of freedom only:

$$\mathbf{q}_c = \mathbf{\Lambda}_L \begin{Bmatrix} \mathbf{q}_L \\ \mathbf{q}_B \\ \mathbf{q}_{LB} \\ \mathbf{q}_I \end{Bmatrix} \tag{5}$$

$$\mathbf{\Lambda}_R\, \mathbf{f}_c = \mathbf{0} \tag{6}$$

Inserting these condensed vectors into Eq.(1), one has:

$$\mathbf{\Lambda}_L\, \mathbf{D}(\omega)\, \mathbf{\Lambda}_R \begin{Bmatrix} \mathbf{q}_L \\ \mathbf{q}_B \\ \mathbf{q}_{LB} \\ \mathbf{q}_I \end{Bmatrix} = \mathbf{A}(\omega, \mu_x, \mu_y)\, \mathbf{u} = \mathbf{0} \tag{7}$$

where the system of equations is condensed to the left-bottom and internal degrees of freedom are represented in vector $\mathbf{u}$.

By solving this eigenvalue problem for each frequency ω, one can find the wave vectors μ_x and μ_y. Because the unit-cell model is not only axisymmetry but also central symmetric, the band structures can be calculated by scanning the wave vectors along the direction of Γ–X–M–Γ in the first irreducible Brillouin zone shown in Fig. 3.

3. NUMERICAL ANALYSIS

The unit cell of the corrugated plate is composed of a shell pyramid whose properties are listed in Table 1 and its geometry is shown in Fig. 5. The plate has a thickness of 1 mm all over the unit cell.

The finite element model of the unit cell is created in the software COMSOL Multiphysics. Triangular shell elements are adopted to model the surfaces of the unit cell (Fig. 4). These elements are linear Mindlin-Reissner shell elements, with three nodes and six degrees of freedom per node (three displacements and three rotations)[1]. An extra fine grid is adopted, thus resulting in models with more than 2,000 elements (the number of elements depends on the aspect ratio of the unit cell).

Flochet boundary conditions are adopted for the free edges of the unit cell to represent the periodicity of the structure. Hence, in this case, the plate is considered infinitely long in both X and Y directions (infinite periodicity). This hypothesis tends to be a good representation of finite structures composed of several unit cells (above 10 unit cells – Sugino *et al.* (2016)).

[1]More information at the website https://doc.comsol.com/5.4/doc/com.comsol.help.sme/sme_ug_shell_plate.08.03.html (accessed in June 2023).

Table 1. Parameters of the model of the corrugated plate.

property	**value**	**unit**
cell height (h)	0 – 10	mm
cell length in X direction (L_x)	30 – 120	mm
cell length in Y direction (L_y)	30 – 120	mm
plate thickness (t)	1	mm
plate Young's modulus (E)	69×10^9	N.m^{-2}
plate density (ρ)	2,700	kg.m^{-3}

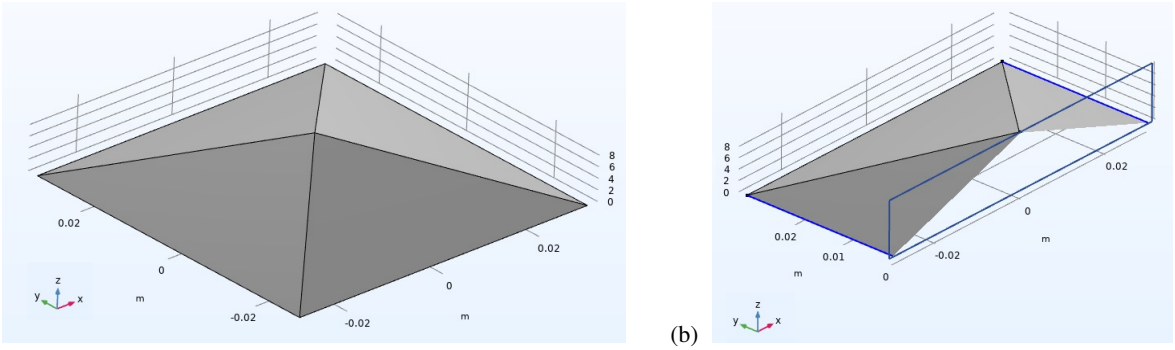

Figure 4. Model of the unit cell of the corrugated plate: (a) unit cell (shell pyramid), (b) section view of the unit cell.

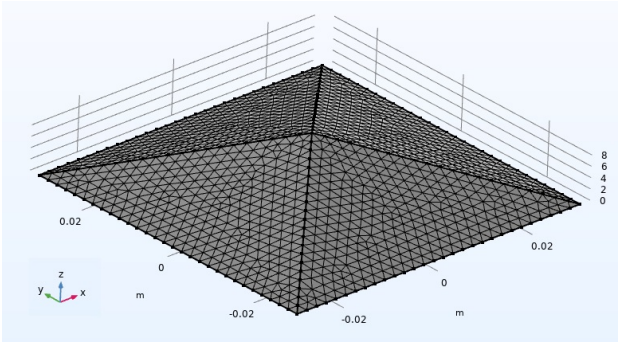

Figure 5. Finite element model of the unit cell.

The eigenfrequency analysis is performed considering the first ten natural frequencies of the system excluding the rigid modes. The dispersion diagrams are obtained by a parametric sweep of the wave vectors in the directions of the irreducible Brillouin zone. Every sweep is divided into 20 steps.

3.1 Variation of the Unit Cell's Height

This first analysis investigates the effect of periodic corrugation on plate dynamics. For that, I consider a squared unit cell (60 × 60 mm) whose height is varied from 0 to 10 mm. For every height condition, the dispersion diagram is built along the Γ-X-M-Γ direction of the irreducible Brillouin zone, and the band gaps are identified based on the frequency regions where the wave vectors are 0 or π. The results are shown in Fig. 6.

As we can see, when the height of the unit cell is zero (flat plate), no band gaps appear in the frequency spectrum of the structure, as expected. However, as the height of the unit cell increases, there appear band gaps in the frequency spectrum of the structure, especially in the X-M direction of the Brillouin zone. In this case, several band gaps appear in different frequency regions of the spectrum, and their bandwidths widen as a function of the cell height.

Some band gaps also appear in the Γ-X direction of the Brillouin zone between 7,000 and 8,000 Hz. However, no band gaps appear in the direction M-Γ, which shows that non-complete band gaps are formed in the corrugated plate in the study. This means that vibration waves can still propagate in the M-Γ direction of the corrugated plate irrespective of their frequency. In the other directions (Γ-X and X-M), the waves cannot propagate if their frequencies coincide with the band gap frequencies.

Hence, these results show that it is possible to create band gaps in plates by corrugating them in a periodic sequence of squared pyramid unit cells. However, the obtained band gaps are non-complete (waves still propagate in certain directions of the irreducible Brillouin zone).

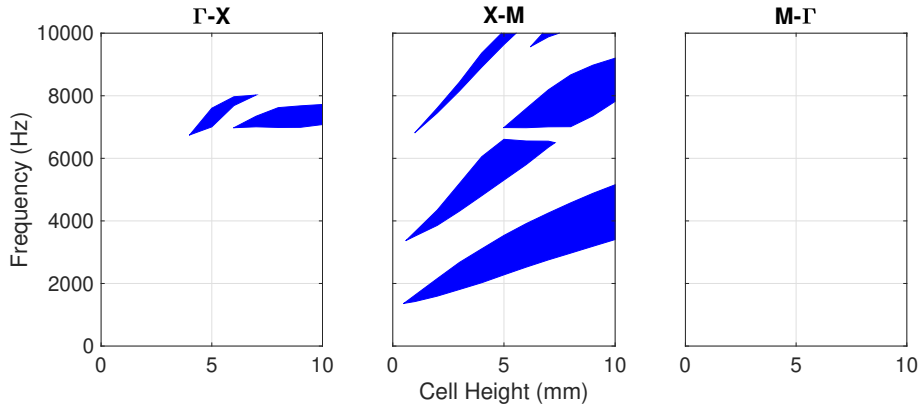

Figure 6. Band gap formation (blue areas) in the frequency spectrum of the corrugated plate as a function of the unit cell height.

3.2 Variation of the Unit Cell's Aspect Ratio

This next analysis investigates the effect of changing the aspect ratio of the unit cell on plate dynamics. For that, I consider a rectangular unit cell, whose height is 10 mm (constant), but the base can vary its aspect ratio between 0.5 to 2. For every aspect ratio condition, the dispersion diagram is built along the Γ-X-M-Γ direction of the irreducible Brillouin zone, and the band gaps are identified based on the frequency regions where the wave vectors are 0 or π.

Figure 7 presents the band gap formation in the structure as a function of the aspect ratio in the X direction. In this case, the length of the unit cell in the Y direction (L_y) is 60 mm and the length in the X direction varies from 30 to 120 mm. As one can see, the aspect ratio changes the central frequency of the band gaps. If the aspect ratio is smaller than 1, the central frequency of the band gaps shifts towards higher frequencies. On the other hand, if the aspect ratio is greater than 1, the central frequency of the band gaps shifts towards lower frequencies. This is probably caused by the resultant variation of the strusture's inertia, which increases as the aspect ratio increases. In addition, one observes in Fig. 7 that the band gaps tend to close as the aspect ratio significantly deviates from 1.

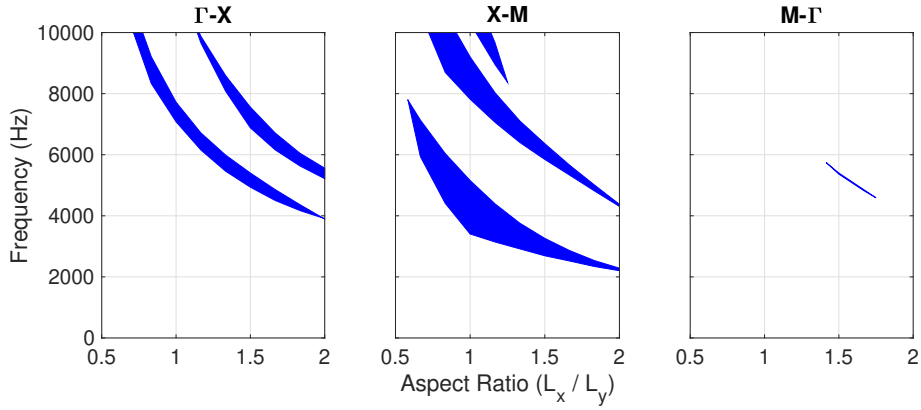

Figure 7. Band gap formation (blue areas) in the frequency spectrum of the corrugated plate as a function of the unit cell aspect ratio (variation of cell length in X direction).

The majority of the band gaps appear in the Γ-X and X-M directions of the Brillouin zone. In this case, there is also a narrow band gap in the M-Γ direction. However, by overlapping the band gap regions of the three directions (Fig. 8), one observes that the band gap regions do not coincide. This shows that the formed band gaps are also non-complete, and waves can propagate in the structure in preferential directions.

Figure 9 presents the band gap formation in the structure as a function of the aspect ratio in the Y direction. In this case, the length of the unit cell in the X direction (L_x) is 60 mm and the length in the Y direction varies from 30 to 120 mm. As one can see, again the aspect ratio changes the central frequency of the band gaps. If the aspect ratio is smaller than 1, the central frequency of the band gaps shifts towards higher frequencies. On the other hand, if the aspect ratio is greater than 1, the central frequency of the band gaps shifts towards lower frequencies. However, the band gaps in this case present larger bandwidths and they do not tend to close for aspect ratios above 1.

Once again, the majority of the band gaps appear in the Γ-X and X-M directions of the Brillouin zone. However, the same narrow band gap in the M-Γ direction appears. In this case, by overlapping the band gap regions of the three directions (Fig. 10), one observes that the band gap regions do coincide in the narrow band gap region in the M-Γ direction.

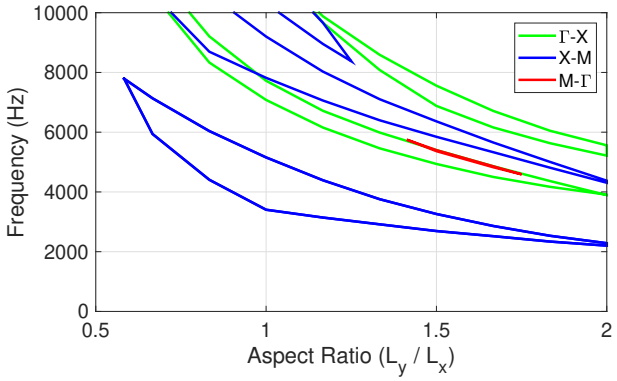

Figure 8. Band gap formation in the frequency spectrum of the corrugated plate as a function of the unit cell aspect ratio (variation of cell length in X direction) – Non-complete band gaps.

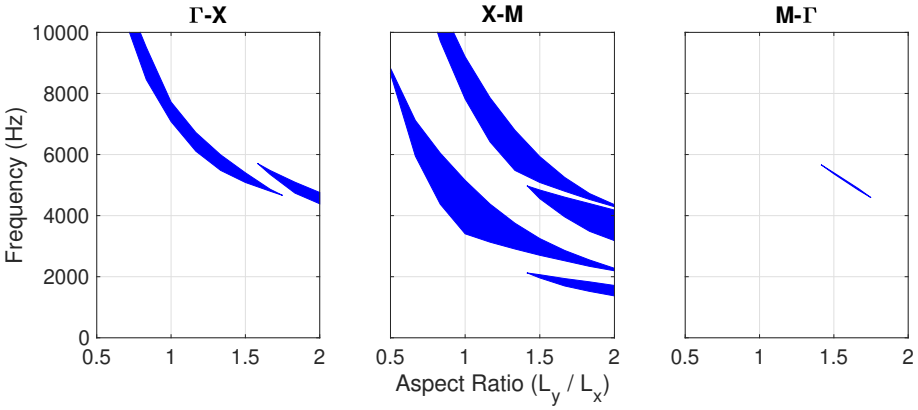

Figure 9. Band gap formation (blue areas) in the frequency spectrum of the corrugated plate as a function of the unit cell aspect ratio (variation of cell length in Y direction).

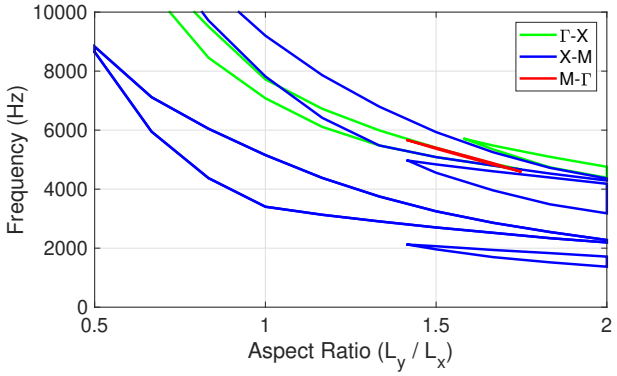

Figure 10. Band gap formation in the frequency spectrum of the corrugated plate as a function of the unit cell aspect ratio (variation of cell length in Y direction) – Formation of a complete band gap.

Although very narrow, a complete band gap formed in the structure by changing the aspect ratio of the unit cell in the Y direction. The wide band gaps in the Γ-X and X-M directions are non-complete though.

Hence, these results show that it is possible to change the band gaps (center frequency and bandwidth) of the corrugated plate by varying the aspect ratio of the pyramid-shaped unit cell. The obtained band gaps are non-complete in general, but it was possible to find a narrow complete band gap by changing the aspect ratio in the Y direction.

4. CONCLUSION

Most of the periodic structures analyzed in the literature involve some sort of modification of the mass or the material property along the structure. In the case of corrugated beams and plates, no such modification is needed, because the beam or plate is shaped in the corrugated geometry, keeping the same material properties and the cross-sectional area along the beam (the geometry does the work). That represents an advantage from a manufacturing standpoint.

Considering this, the present work presented an analysis of the band gap formation in corrugated plates. In this case,

the 2D structure (plate) was corrugated with straight faces, thus resulting in a periodic sequence of pyramid-shaped bumps. The corrugated plate was modeled by finite elements and the resultant dispersion diagrams (out-of-plane vibration) were obtained using the COMSOL software. The results showed that:

- it is possible to create band gaps in plates by corrugating them in a periodic sequence of squared pyramid unit cells. However, the obtained band gaps are non-complete (waves still propagate in certain directions of the irreducible Brillouin zone). The center frequency and the bandwidth of the gaps tend to increase as the unit cell's height increases;
- it is possible to change the band gaps (center frequency and bandwidth) of the corrugated plate by varying the aspect ratio of the pyramid-shaped unit cell. If the aspect ratio is smaller than 1, the central frequency of the band gaps shifts towards higher frequencies. On the other hand, if the aspect ratio is greater than 1, the central frequency of the band gaps shifts towards lower frequencies. In addition, the band gaps tend to close as the aspect ratio significantly deviates from 1;
- the band gaps obtained by varying the aspect ratio of the unit cell are still non-complete in general, but it was possible to find a narrow complete band gap by changing the aspect ratio in the Y direction.

5. ACKNOWLEDGEMENTS

This work was funded by CNPq (Conselho Nacional de Desenvolvimento Científico e Tecnológico) under grant number 304212/2021-0, and FAPESP (Fundação de Amparo à Pesquisa do Estado de São Paulo) under grant number 2018/15894-0 (Projeto ENVIBRO).

6. REFERENCES

Bachour, R.S. and Nicoletti, R., 2021. "Natural frequencies and band gaps of periodically corrugated beams". *Journal of Vibration and Acoustics*, Vol. 143, No. 4, p. 044502.

Casadei, F., Ruzzene, M., Dozio, L. and Cunefare, K.A., 2010. "Broadband vibration control through periodic arrays of resonant shunts: experimental investigation on plates". *Smart Materials and Structures*, Vol. 19, No. 1, p. 015002.

Das, S., Dwivedi, K., Rajasekharan, S.G. and Rao, Y.V.D., 2020. "Vibration attenuation and bandgap characteristics in plates with periodic cavities". *Journal of Vibration and Control*, Vol. 27, No. 7-8, pp. 827–838.

El-Sabbagh, A., Akl, E. and Baz, A., 2008. "Topology optimization of periodic mindlin plates". *Finite Elements in Analysis and Design*, Vol. 44, No. 8, pp. 439–449.

Guo, W., Nie, R., Zhu, X., Mao, Y., Song, L. and Zhang, H., 2022. "Flexural wave band gaps in periodic bi-directionally orthogonal stiffened plates with holes". *International Journal of Structural Stability and Dynamics*, Vol. 22, No. 16, p. 2250183.

Nouh, M.A., Aldraihem, O.J. and Baz, A., 2016. "Periodic metamaterial plates with smart tunable local resonators". *Journal of Intelligent Material Systems and Structures*, Vol. 27, No. 3, pp. 1829–1845.

Poggetto, V.F. and Arruda, J.R.F., 2021. "Widening wave band gaps of periodic plates via shape optimization using spatial fourier coefficients". *Mechanical Systems and Signal Processing*, Vol. 147, p. 107098.

Ruzzene, M., Mazzarella, L., Tsopelas, P. and Scarpa, F., 2002. "Propagation in sandwich plates with periodic auxetic core". *Journal of Intelligent Material Systems and Structures*, Vol. 13, No. 9, pp. 587–597.

Song, Y., Feng, L., Wen, J., Yu, D. and Wen, X., 2015. "Analysis and enhancement of flexural wave stop bands in 2d periodic plates". *Physics Letters A*, Vol. 379, No. 22-23, pp. 1449–1456.

Sugino, C., Leadenham, S., Ruzzene, M. and Erturck, A., 2016. "Mechanics of bandgap formation in locally resonant finite elastic metamaterials". *Journal of Applied Physics*, Vol. 120, No. 13, p. 134501.

Wang, J., Wen, W.J. and Wen, X., 2012. "Flexural vibration band gaps in periodic stiffened plate structures". *Mechanika*, Vol. 18, No. 2, pp. 186–191.

Xiong, Y., Xu, A., Wen, S., Li, F. and Hosseini, S.M., 2023. "Optimization of vibration band-gap characteristics of a periodic elastic metamaterial plate". *Mechanics of Advanced Materials and Structures*, Vol. 30, No. 15, pp. 3204–3214.

Zhang, H., Chen, J. and Han, X., 2012. "Lamb wave band gaps in a homogenous plate with periodic tapered surface". *Journal of Applied Physics*, Vol. 112, No. 5, p. 054503.

Zhou, H., Zhao, T., Wu, H. and Meng, J., 2020. "The vibroacoustic analysis of periodic structure-stiffened plates". *Journal of Sound and Vibration*, Vol. 481, p. 115402.

Zouari, S., Genevaux, J.M., Brocail, J. and Ablitzer, F., 2017. "Band gap formation in thin plates with a periodic array of resonators". *Mechanics and Industry*, Vol. 18, No. 3, p. 304.

7. RESPONSIBILITY NOTICE

The author is solely responsible for the printed material included in this paper.